Received: 20 February 2020 | Revised: 15 June 2020 | Accepted: 19 June 2020

DOI: 10.1111/exd.14135

REGULAR ARTICLE

Experimental Dermatology WILEY

Biological effects of a new ultraviolet A_1 prototype based on light-emitting diodes on the treatment of localized scleroderma

Stephanie Arndt | Clara Lissner | Petra Unger | Wolfgang Bäumler | Mark Berneburg | Sigrid Karrer

Department of Dermatology, University Medical Center Regensburg, Regensburg, Germany

Correspondence
Stephanie Arndt, Department of Dermatology, University Medical Center Regensburg, Franz Josef Strauss Allee 11, 93053 Regensburg, Germany.
Email: stephanie.arndt@ukr.de

Funding information
This research did not receive any specific grant from funding agencies in the public, commercial or not-for-profit sectors.

Abstract

Ultraviolet A_1 (UVA_1) phototherapy (spectral range 340-400 nm) is a well-established treatment option for various skin diseases such as localized scleroderma. Recent improvements of conventional UVA_1 light sources (metal-halide or fluorescent lamps) have brought attention to a new light-emitting diode (LED) technology with remarkable advantages in handling and clinical routine. This study provides a preclinical histological and molecular evaluation of an LED-based UVA_1 prototype with a narrower spectral range (360-400 nm) for treating localized scleroderma. Scleroderma mouse models and fibroblasts in vitro were exposed to LED-based UVA_1 phototherapy or to irradiation with a commercially available metal-halide lamp emitting low-dose (20, 40 J/cm^2), medium-dose (60 J/cm^2) and high-dose (80, 100 J/cm^2) UVA_1 light. Both UVA_1 light sources affected inflammatory genes (IL-1α and IL-6) and growth factors (TGFß-1 and TGFß-2). Increased collagen type 1 was reduced after UVA_1 phototherapy. Matrix metalloproteinase-1 was more enhanced after a medium dose of LED-based UVA_1 phototherapy than after conventional treatment. In vivo, dermal thickness and the amount of collagen were reduced after both treatment methods. Remarkably, myofibroblasts were more effectively reduced by a medium dose of LED-based UVA_1 phototherapy. The study indicates that LED-based UVA_1 phototherapy yields similar or even better results than conventional treatment. In terms of biosafety and patient comfort, LED-based UVA_1 phototherapy offers clear advantages over conventional treatment because of the use of a narrower and less harmful UVA_1 spectrum, less heat generation and shorter treatment times at the same irradiation intensity. Clinical studies are required to confirm these results in patients with localized scleroderma.

KEYWORDS

extracellular matrix, fibroblasts, LED-based UVA_1, localized scleroderma, phototherapy

Stephanie Arndt and Clara Lissner are equally contributed.

1 | INTRODUCTION

Localized scleroderma (LS) is a distinctive inflammatory disease that leads to sclerosis of the skin and subcutaneous tissues.[1-4] Management of LS is difficult, and no causal therapy is available so far. Topical and systemic immunosuppressants such as corticosteroids are commonly used as anti-fibrotic agents but with considerable side effects and limited efficacy.[5,6] The beneficial effects of different forms of phototherapy in the treatment of LS have been described in many studies.[7-13] The development of UVA_1 phototherapy (340-400 nm) has highly improved treatment of LS.[14,15] Because UVA_1 light is less erythematogenic than broadband UVA, it is possible to apply much higher doses of UVA_1 without the risk of sunburn.UVA_1 light penetrates deeper into the skin than UVB and UVA_2.[16] In the first prospective study on LS, high-dose UVA_1 light (130 J/cm^2) was highly effective in reducing skin sclerosis, and some patients even showed complete clearance.[11] Lower UVA_1 doses (30 J/cm^2) were also highly effective and well-tolerated by patients with LS who showed a significant reduction in skin thickness.[17]

Commercially available UVA_1 light sources for therapeutic use are fluorescent lamps (ie TL10R 100W, Philips) or high-output metal-halide lamps (ie Sellamed 4000W, Sellas Medizinische Geräte GmbH). Low-dose to medium-dose UVA_1 phototherapy is usually conducted by means of fluorescent lamp cubicles, that is full-body UV cabins, allowing the irradiation of large body areas; in contrast, metal-halide lamps are more often used for high-dose UVA_1 treatments.[14,18,19] Despite the therapeutic success of conventional lamps in the treatment of LS, these light sources should be further developed in terms of biosafety and patient comfort. For patients, conventional therapy involves long irradiation times per therapy session (up to 60 minutes) and treatment durations (up to 40 sessions) as well as possible discomfort due to severe heat from the light sources (up to 40°C). The new light-emitting diode (LED) technology provides remarkable advantages over conventional treatment. The higher power of the LEDs significantly reduces the treatment time per session. Furthermore, LEDs only develop very low waste heat. LED technology also allows the manufacturing of small hand-operated UVA_1 devices that require less space. In this way, only skin areas requiring treatment may be targeted. Irradiation of healthy tissue can be avoided when only circumscribed areas need to be treated. The narrower UVA_1 spectrum due to the mixture of different LEDs is also of importance. Patient safety could be improved by eliminating potentially more damaging short-wave UVA_1 radiation (340-360 nm). This study investigated the—so far—unresolved question whether molecular or cellular mechanisms are affected by the different UV spectrum.

2 | METHODS

2.1 | Cell culture

The in vitro study included human dermal fibroblasts from $n = 6$ different donors (#231340, #7F3943, #7F3950, #2F0621, #9F0438 and #9F0889) purchased from CellSystems® (Biotechnologie Vertrieb GmbH). Fibroblasts were maintained in Dulbecco's modified Eagle's medium (DMEM) (Thermo Fisher Scientific) and supplemented with 10% fetal bovine serum (both from PAN Biotech) and 1% penicillin-streptomycin, as well as 1% L-glutamine (both from Sigma-Aldrich). All cells were cultured in 75 cm^2 Falcon™ Flasks (Corning Inc), incubated under humid conditions in a 5% CO_2 incubator at 37°C and split 1:3 every 3 days.

2.2 | Animals and treatment groups

The mouse experiments were conducted with129Sv/Ev male mice (original strain from Robertson Lab of Dunn School Pathology of the University of Oxford, UK). All animals ($n = 6$ animals per group) were between 6 and 8 weeks old at the start of the study and were divided into experimental groups according to their cage occupation. Mice were maintained under specific pathogen-free and controlled conditions (22°C, 55% humidity and 12 hours day/night rhythm) and had free access to water and chow. They received human care in compliance with the guidelines outlined in the Guide for the Care and Use of Laboratory Animals. The backs of the mice were shaved (2 × 2 cm^2). The animals were subjected to a well-established bleomycin-induced scleroderma model[20-23] based on the study by Yamamoto et al on BALB/C mice[23] with small modifications adapted for the 129Sv/Ev mouse strain. Mice in the experimental groups (group 2-6) received local subcutaneous injections of 100 µL bleomycin (500 µg/mL; Hexal AG Holzkirchen) five times a week within 6 weeks as well as further injections 1-2 times per week (over the 6 weeks of phototherapy) to maintain the local sclerosis status. Control group 1 received subcutaneous injections of 100 µl of phosphate-buffered saline (PBS) (Sigma-Aldrich) instead of bleomycin (Table S1). To induce a comparable level of local fibrosis that was as homogeneous as possible, the injections were always given by the same person. Groups 3-6 received phototherapeutic treatment for 30 days (5 times per week). The high-dose UVA_1 groups (groups 3 and 4) were treated for 3330 minutes (= 100 J/cm^2) per session and the medium-dose UVA_1 groups (groups 5 and 6) for 2000 minutes (= 60 J/cm^2). Groups 3 and 5 were exposed to irradiation with the metal-halide lamp and groups 4 and 6 to irradiation with the LED prototype (Table S1). The mice were treated in their usual cages to avoid any additional stress. After UVA_1 therapy, all animals were killed by cervical dislocation, and the bleomycin-treated or PBS-treated skin area was removed and subdivided for histological preparation or molecular biological examination.

2.3 | UVA_1 devices, illumination set-up, and treatment of cells and mice

This UVA_1 phototherapy study included two UVA_1 devices (Figure S1A,B) that differed with regard to the type of lamp and the UVA_1

spectrum (Figure S1C). Besides the conventionally used UVA_1 device (340-400 nm) with an installed metal-halide lamp (exposure area of 25 × 25 cm), the study used a UVA_1 prototype (360-400 nm) with light-emitting diode-based technology (exposure area of 30 × 30 cm with 144 single LEDs) (both from Sellas Medizinische Geräte GmbH). Both UVA_1 light sources were positioned and installed to emit the same irradiation power of 50 mW/cm^2. During the UVA_1 treatments, the distance between the metal-halide lamp and the animal cage was 2 cm and between the LED-based UVA_1 prototype and the cage 60 cm.

For UVA_1 treatment, 50 000 cells were seeded onto 6-well cell culture plates and irradiated with different doses of UVA_1 light (20 J/cm^2 - 640 minutes; 40 J/cm^2 - 13 20 minutes; 60 J/cm^2 - 20 00 minutes; 100 J/cm^2 - 33 30 minutes). During UVA_1 irradiation, cells were maintained in 2 ml of phosphate-buffered saline (PBS) (Sigma-Aldrich). Untreated control cells and UVA_1-treated cells simultaneously underwent a change in medium (2 mL DMEM) immediately after irradiation. Cells were incubated for 6 and 24 hours after UVA_1 treatment followed by RNA isolation.

Mice received a medium dose (60 J/cm^2 - 20 00 minutes) and a high dose (100 J/cm^2 - 3330 minutes) of UVA_1 irradiation dependent on their assigned experimental group (Table S1).

Both the in vitro and the in vivo studies were conducted with the two UVA_1 light sources (a metal-halide UVA_1 lamp and the LED-based UVA_1 prototype) under the same conditions to allow a direct comparison. The only difference in the set-up was the use of a fan in the experiment with the metal-halide lamp to protect the animals from severe heat.

2.4 | RNA isolation and reverse transcription

Cellular RNA was isolated using the NucleoSpin® RNA Kit (Macherey-Nagel) according to the manufacturer's instructions. 2 µg of RNA was then transcribed into cDNA by reverse transcriptase reaction using the Super Script™ II Kit (Invitrogen, Thermo Fisher Scientific).

2.5 | Quantitative real-time PCR analysis

Cellular gene expression analysis consisted of quantitative real-time PCR with specific sets of primers (Sigma-Aldrich) and conditions (Table S2) using LightCycler technology (Roche Diagnostics) as described elsewhere.[24] PCR reactions were evaluated by melting curve analysis. ß-actin was amplified to ensure cDNA integrity and to normalize expression. Each real-time PCR was repeated at least 3 times.

2.6 | Enzyme-linked immunosorbent assay (ELISA)

Cell supernatants were collected 48 hours after UVA_1 treatment and of untreated control fibroblasts and were analysed by total MMP-1 ELISA, respectively, according to the manufacturer's instruction. The human total MMP-1 ELISA (DuoSet ELISA Development System) was received from R&D Systems, Wiesbaden-Nordenstadt, Germany, and detects active and pro-Matrix Metalloproteinase-1. Each supernatant was assayed in duplicates, and the entire experiments were performed three times with dermal fibroblasts from $n = 6$ different donors.

2.7 | MTT assay

The 3-[4,5-dimethylthiazol-2-yl]-2,5-diphenyl-tetrazolium bromide (MTT) test is based on the reduction in tetrazolium salt by mitochondrial enzymes to form coloured formazan as an indicator of vitality.[25] To evaluate the cell vitality of human fibroblasts ($n = 6$) after UVA_1 treatment, 10^4 cells/well were seeded onto a 96-well microtitre plate and irradiated with different doses of UVA_1 light (20 J/cm^2 - 640 minutes; 40 J/cm^2 - 1320 minutes; 60 J/cm^2 - 20 00 minutes; 80 J/cm^2 - 2640 minutes; 100 J/cm^2 - 3330 minutes) or remained untreated. During UVA_1 irradiation, cells were maintained in 100 µL of PBS. After irradiation, PBS was replaced by 100 µL of DMEM, and the microtitre plate was incubated under humid conditions in a 5% CO_2incubatorat 37°C for 24 hours. 10 µL of MTT reagent (5 mg/mL in PBS, Sigma-Aldrich) was added directly to the medium in the wells of the microtitre plate and incubated for 4 hours. Insoluble formazan was formed in the cells in proportion to the activity of the dehydrogenases. The formazan was finally dissolved in 100 µL 20% SDS (sodium dodecyl sulphate, Sigma-Aldrich) and incubated overnight in the incubator. Absorbance of the dissolved solution was observed with a microtitre plate reader (MWG-Biotech) at 540 nm. Each sample was assayed in duplicates, and the entire experiments were conducted three times.

2.8 | Histochemical analysis

Immunohistochemistry was conducted on formalin-fixed and paraffin-embedded full-skin preparations from all mice ($n = 6$ mice per group). Skin sections measuring 2 µm were stained with anti-alpha-smooth muscle actin (anti-α-SMA) antibody (EPR5368) (1:1000; Abcam) according to the following protocol: sections were deparaffinized, rehydrated and placed into a steamer in Tris/EDTA buffer (pH 8) for 30 minutes. After cooling down to room temperature, the tissue slides were washed in PBS, incubated with the primary antibody at room temperature for 1 hour, washed again with PBS and incubated with Histofine solution (Nichirei Biosciences INC. Tokyo, Japan) for 30 minutes. Tissue slides were washed again with PBS and incubated with AEC substrate chromogen (ready to use; Dako-Agilent) at room temperature in the dark for 15 minutes. The staining reaction was stopped with H_2O, and counterstaining was done with haematoxylin (Roth).

H&E staining on murine skin sections was done as described previously.[26] Extracellular matrix accumulation in skin sections was

determined by staining with Sirius red/fast green.[27] The intensity of the Sirius red staining of the murine tissue sections was quantified with the image J software (http://www.imagej.softonic.de) and expressed as a percentage of the total area. All tissue slides were scanned with a histo-scanner (PreciPoint, M8), and representative pictures were visualized.

2.9 | Analysis of collagen content

Collagen in mouse tissues was analysed with the QuickZyme collagen assay according to the manufacturer's instructions (QuickZyme Biosciences).

2.10 | Statistical analysis

Data are expressed as mean values ± standard deviation (SD). Data were analysed with GraphPad Prism 5 software (GraphPad Software Inc). Groups were compared by one-way ANOVA with Tukey's honestly significant difference (HSD) post hoc test analysis. Differences were considered statistically significant at $P < .05$.

2.11 | Study approval

The animal study was conducted according to the NIH Guide for the Care and Use of Laboratory Animals, with the appropriate permission from the Animal Rights Commission of the State of Bavaria, and approved by the Committee on the Ethics of Animal Experiments of the University of Regensburg, Germany (permit number 55.2 DMS-2532-2-461).

3 | RESULTS

The study purpose was to evaluate molecular and histological effects of an LED-based UVA_1 prototype (spectral range 360-400 nm) on human fibroblasts and dermal fibrosis in a bleomycin-induced mouse model of scleroderma in comparison to conventional UVA treatment with a high-pressure metal-halide lamp (spectral range 340-400 nm). For the in vitro approach, different UVA_1 dose regimens (20, 40, 60, 80 and 100 J/cm^2) were evaluated, and for the in vivo approach 2 different treatment regimens (high dose: 100 J/cm^2 and medium dose: 60 J/cm^2).

3.1 | UVA_1 phototherapy equipment and emission spectrum

Figure S1 shows the exposure unit and the emission spectrum of the UVA_1 metal-halide high-pressure lamp (SELLASOL) (Figure S1A, C) and the LED-based UVA_1 prototype (Figure S1B,C).

3.2 | Examination of morphology and cell vitality of human fibroblasts after UVA_1 treatment

To compare the two UVA_1 light sources with respect to cell viability, cell morphology and cell vitality were determined 24 hours after UVA_1 treatment by means of an MTT test. Human fibroblasts exposed to high UVA_1 doses (80 and 100 J/cm^2) appeared swollen, broken and round, and the damage was most critical after treatment with either light source (Figure 1A). Single UVA_1 treatments with up to 60 J/cm^2 did not change the morphology of the fibroblasts. Cell vitality significantly decreased with increasing UVA_1 doses (Figure 1B). Doses > 60 J/cm^2 were defined as the irradiation limit for both UVA_1 light sources and were not used in further cell culture experiments.

3.3 | Effects of UVA_1on cytokines, growth factors and collagen metabolism in fibroblasts

mRNA expression of IL-1α and IL-6, which was initially analysed 6 hours after exposure to UVA_1, was induced after treatment with both the metal-halide lamp and the LED-based prototype in comparison with untreated control. mRNA expression did not seem to be dependent on the UVA_1 dose (Figure 2A,B). Interestingly, induction of IL-1α was significantly higher with the LED-based UVA_1 prototype at the low dose of UVA_1 of 20 J/cm^2. Next, the mRNA expression levels of matrix metalloproteinase-1 (MMP-1), collagen type 1 (Col-1), and transforming growth factor ß-1 and transforming growth factor ß-2 (TGFß-1 and TGFß-2) were examined 24 hours after UVA_1 exposure. MMP-1 mRNA expression had increased after UVA_1 treatment with the highest induction at the UVA_1 dose of 60 J/cm^2 for either light source. Here, the LED-based prototype showed a significant induction advantage (Figure 2C). Investigations of MMP-1 at the mRNA level were supplemented with data showing the human total MMP-1 (human active MMP-1 and pro-MMP-1) in cell culture supernatants collected 48 hours after UVA_1 treatment. The results showed that in the supernatants collected from UVA_1-treated fibroblasts significantly more total MMP-1 protein can be detected when using a UVA_1 dose of 40 or 60 kJ/cm^2 compared to the untreated control (Figure S2). In analogy to the mRNA data, a dose of 60 kJ/cm^2 also showed a significantly increased amount of total MMP-1 protein in the supernatant when using the LED UVA_1 device compared to the metal-halide lamp. The expression of Col-1 was significantly down-regulated at doses ≥40 J/cm^2. Lower UVA_1 doses with either light source did not seem to have any reducing effect on the mRNA expression level of Col-1 (Figure 2D). Expression of TGFß-1 was induced after UVA_1 irradiation of normal human fibroblasts compared to untreated cells (Figure 2E). Interestingly, mRNA induction seemed to be dose-dependent for metal-halide UVA_1 treatment and not dose-dependent for LED-based UVA_1 treatment. In contrast, TGFß-2 was down-regulated with the strongest effect at the dose of 60 J/cm^2 for either light source (Figure 2F). In summary, these results indicate that both UVA_1 light sources affect identical biological mechanisms in fibroblasts with similar or even better effects of the new LED-based light

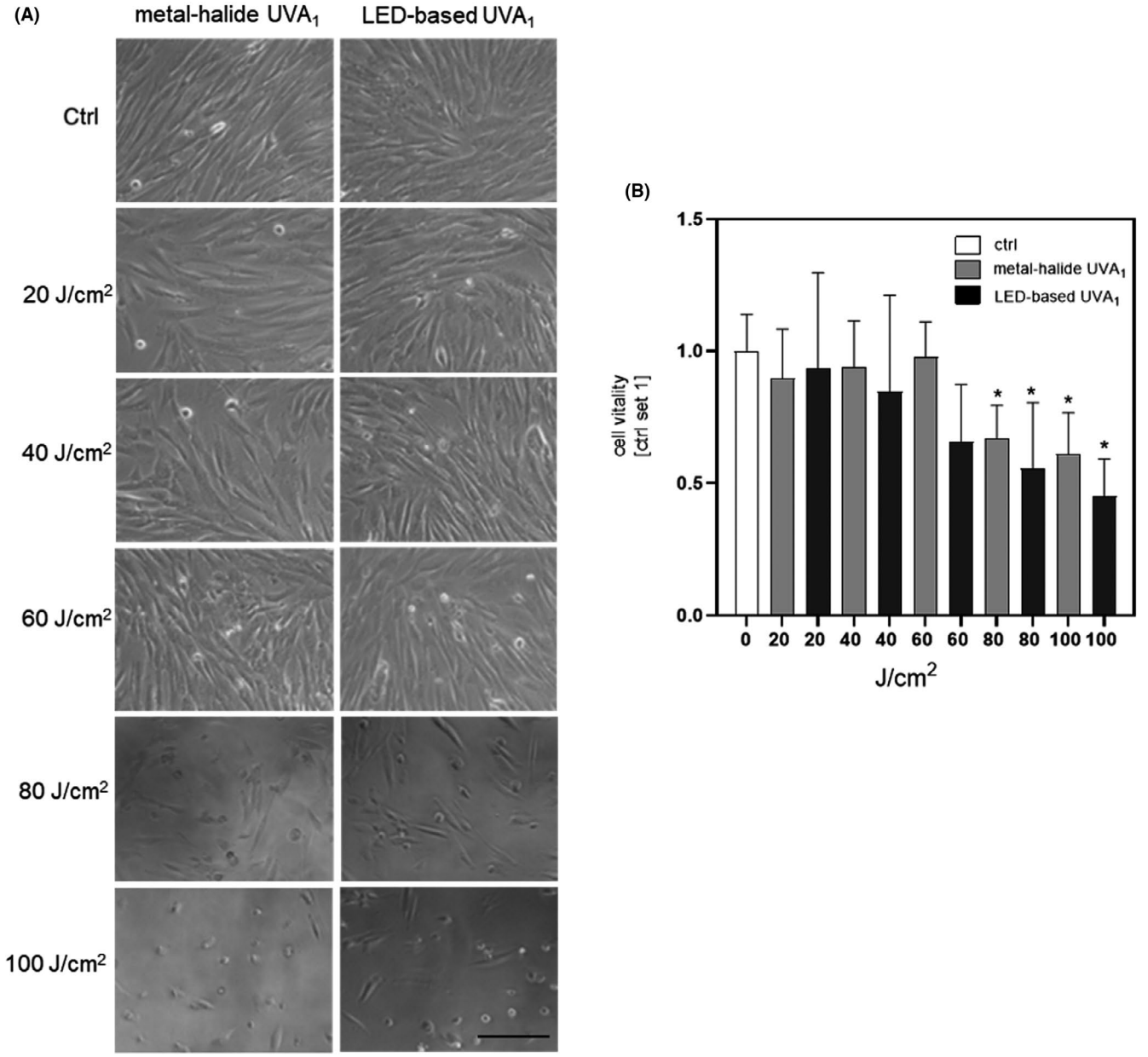

FIGURE 1 Morphology and vitality of fibroblasts after UVA_1 treatment. A, Fibroblasts (#9F0438 as example) were exposed to different UVA_1 doses (20, 40, 60, 80, and 100 J/cm^2) or remain untreated (ctrl.; 0 J/cm^2). Cells treated with high UVA_1 doses (80 and 100 J/cm^2) appeared swollen, broken and round. Scale bar: 500 μm. B, Cell vitality (MTT test) significantly decreased with increasing UVA_1 doses (fibroblasts from $n = 6$ different donors) (*$P < .05$, ANOVA with Tukey's multiple comparison test). No significant differences were found between the two light sources

source with a UVA_1 spectrum (340-400 nm) that is 20 nm narrower than that of the conventional metal-halide lamp (460-400 nm).

3.4 | Evaluation of dermal thickness, collagen content and the number of α-SMA–positive myofibroblasts after UVA_1 treatment

The biological effects of the two UVA_1 light sources were compared by means of a well-established bleomycin-induced murine scleroderma model in a preclinical in vivo approach.[23] After 30 subcutaneous bleomycin injections, the mice had developed dermal sclerosis and were divided into different phototherapeutic treatment groups (Table S1). UVA_1-treated groups (groups 3-6) received 30 UVA_1 irradiation sessions and 10 additional bleomycin injections to maintain the status of sclerosis. The mean dermal thickness of the bleomycin control group 2, which contains 30 bleomycin injections and 10 additional bleomycin injections to maintain the status of sclerosis was 550.81 μm (Std. D. ± 102.8) in comparison with 186.51 μm (SD ± 34.8) in the group of healthy mice (group 1). Dermal thickness was significantly reduced after high-dose (100 J/cm^2) UVA_1 treatment with the metal-halide lamp

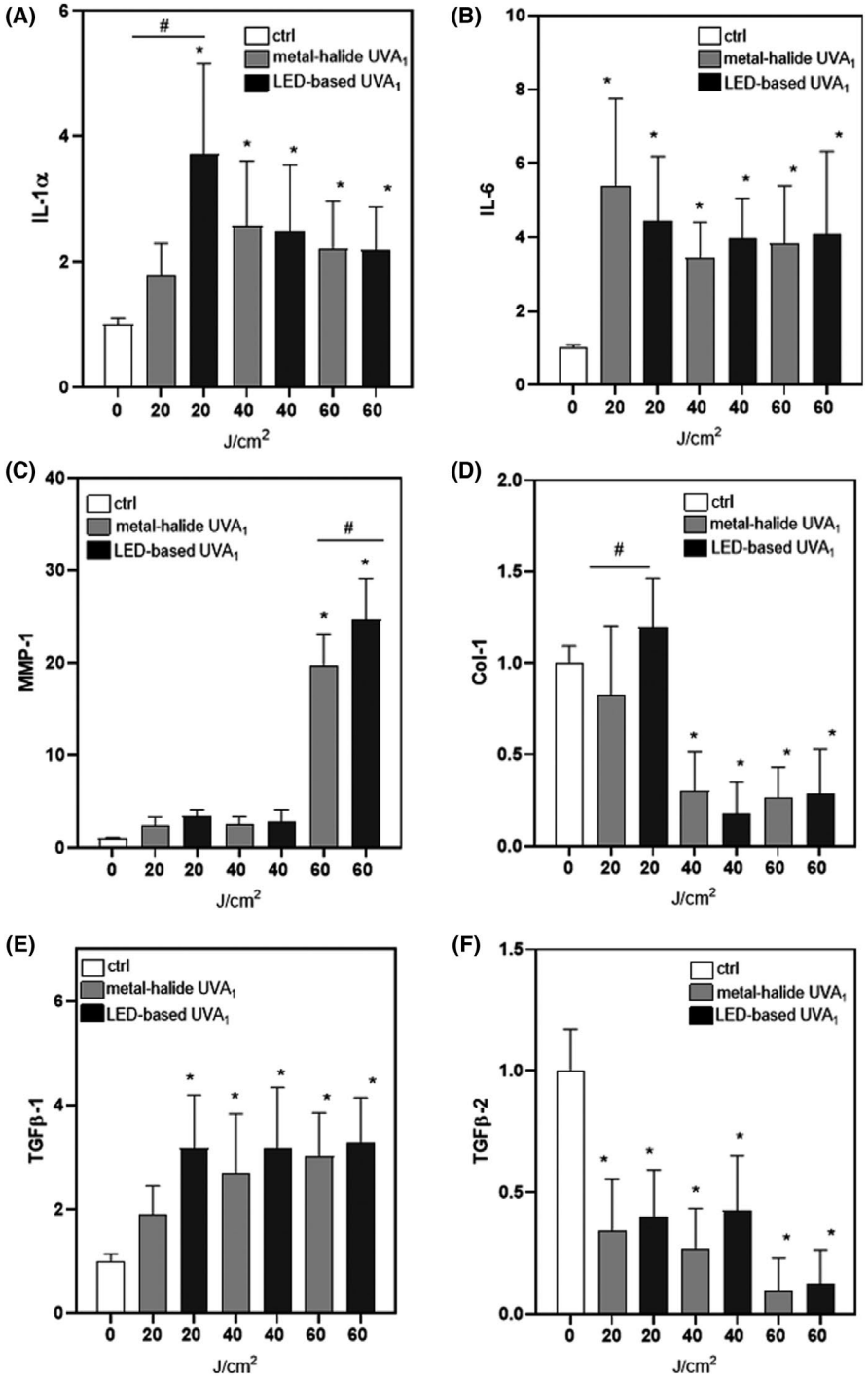

FIGURE 2 Gene expression marker analyses in human fibroblasts after UVA_1 treatment. Different fibroblasts ($n = 6$ different donors) were exposed to UVA_1 (metal-halide UVA_1 or LED-based UVA_1) using different treatment regimens (20, 40 and 60 J/cm^2) or remain untreated (ctrl.; 0 J/cm^2). RNA was isolated 6 or 24 h after treatment as indicated in the text, and different sclerosis-related molecular markers were analysed. A, IL-1α, (B) IL-6, (C) MMP-1, (D) Col-1, (E) TGFß-1 and (F) TGFß-2 (*#$P < .05$, ANOVA with Tukey's multiple comparison test)

(group3: 426.10 μm; SD ± 58.6) and the LED-based UVA_1 prototype (group 4:413.10 μm; SD ± 31.2) in comparison with group 2 (Figure 3A). Dermal thickness was also reduced after medium-dose UVA_1 treatment regimens, but the reduction was not significant with either light source in comparison with the untreated group 2 (group 5:446.20 μm; SD ± 80.70; group 6:441.30 μm; SD ± 56.4). The collagen content in the affected skin after UVA_1 treatment was histologically analysed by means of Sirius red/fast green staining (Figure 4B) and image analysis (Figure 3B) and quantified using a hydroxyproline assay (Figure 3C). The amount of collagen was reduced after each UVA_1 treatment regimen; however, compared to the bleomycin-only group (group 2), the reduction was only significant after high-dose treatment with either light source (Figure 3C). Finally, the number of α-SMA–positive myofibroblasts was determined by a dermato-histopathologist. Myofibroblasts were significantly reduced after high-dose UVA_1 treatment with the metal-halide lamp and medium-dose UVA_1 treatment with the LED-based UVA_1 prototype (Figure 3D). The obviously stronger α-SMA staining in groups 3-6 (Figure 4C) was due to the blood vessels that were also α-SMA positively stained and whose synthesis is known to increase after UVA_1 irradiation.[28] In summary, these in vivo results indicate that both UVA_1 light sources are effective

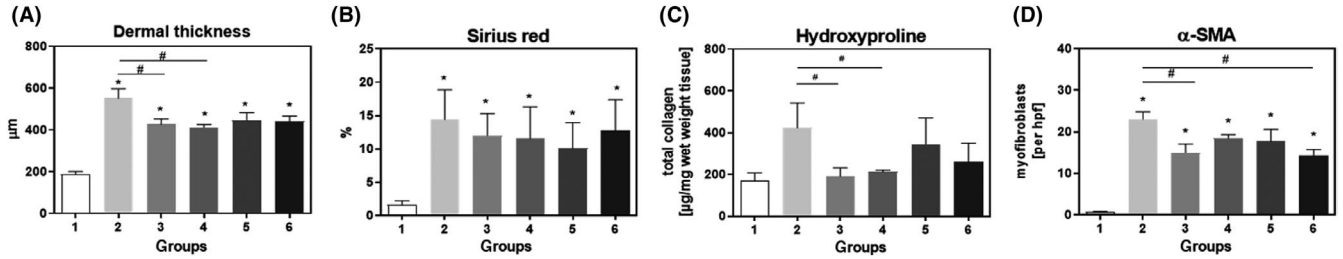

FIGURE 3 Evaluation of dermal thickness, collagen content and the number of α-SMA–positive myofibroblasts in a bleomycin-induced scleroderma model after UVA_1 treatment. A, Dermal thickness was determined in µm in the 6 mice groups. Representative images of mice ($n = 6$ mice per group) were taken, and 5 measurements per image were used for the calculation ($^{*\#}P < .05$, ANOVA with Tukey's multiple comparison test). B, Determination of the fibrotic region by quantifying the Sirius red-positive area by image analysis ($^{*}P < .05$, ANOVA with Tukey's multiple comparison test). C, Protein quantification of total collagen in the dermis within the 6 mice groups ($n = 6$ mice per group) ($^{*}P < .05$, ANOVA with Tukey's multiple comparison test). D, Quantification of α-SMA–positive fibroblasts (myofibroblasts) (average of three hpf/animal; $n = 6$ animals per group) ($^{*\#}P < .05$, ANOVA with Tukey's multiple comparison test). SMA, smooth muscle actin; hpf, high-power field

FIGURE 4 Histological overview of the bleomycin-induced scleroderma model after UVA_1 treatment. Representative images of (A) H&E, (B) Sirius red/fast green and (C) α-SMA–stained sections of local skin fibrosis in different treatment groups (group 1: healthy control; group 2: bleomycin (Bleo) control; group 3: metal-halide UVA_1 (100 J/cm^2); group 4: LED UVA_1 (100 J/cm^2); group 5: metal-halide UVA_1 (60 J/cm^2); and group 6: LED-based UVA_1 (60 J/cm^2). α-SMA–stained vessel structures are strongly increased after UVA_1 treatment and are marked with dotted arrows in the enlarged sections. Full arrows in the enlarged sections indicate α-SMA positively stained fibroblasts. Scale bars: 500 µm

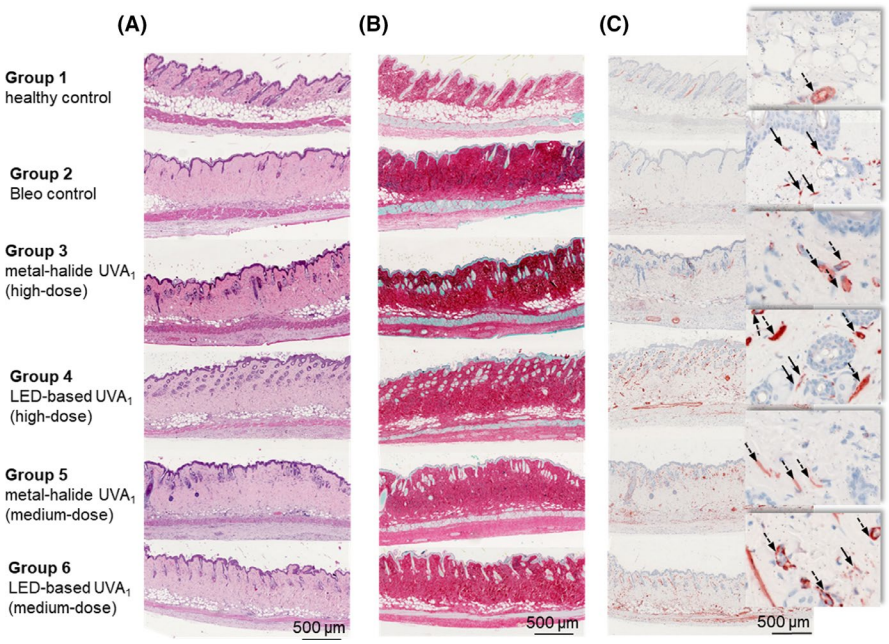

in reducing sclerosis in localized scleroderma with minor differences according to the dose of UVA_1 irradiation applied.

4 | DISCUSSION

The aim of this study was to evaluate the impact of a new LED-based UVA_1 prototype with a spectral range of 360 to 400 nm on the treatment of LS. Normal human fibroblasts and a dermal fibrosis mouse model were used for analysis. In terms of biosafety and patient comfort, LED-based UVA_1 light technology offers clear advantages over conventional metal-halide lamps with a broader spectral range of 340 to 400 nm. Next to the narrower and less harmful UVA_1 spectrum, the LED-based UVA_1 prototype has the advantage of less heat development and shorter treatment times at the same irradiation intensity.[29] However, the molecular and histological effects are also decisive when comparing different UVA_1 light sources. Therefore, we analysed the effects on cell morphology, cell vitality, gene expression of sclerosis-relevant marker molecules, dermal thickness, collagen content and the status of myofibroblast activation in vivo.

First of all, we focused on the morphology and vitality of normal human fibroblasts. Different UVA_1 doses (20, 40, 60, 80 and 100 J/cm^2) were examined, and morphological changes (swollen, broken and round) were observed at doses of 80 J/cm^2 and higher. No morphological differences were found between the conventional lamp and the LED-based prototype. Cell vitality decreased dose-dependently and was significantly reduced after doses of 80 J/cm^2 and higher with either light source. Hereby, the narrower UVA_1 spectrum of the LED-based UVA_1 prototype did not seem to affect cell vitality. Up to date, only a few murine studies are available using a narrowband UVA_1 light source for the treatment of scleroderma.[30,31] Karpec and coauthors described the safety and efficacy of 365 nm LED-based UVA_1 phototherapy in bleomycin-induced scleroderma in

mice,[31] but the optimum UVA_1 spectrum for scleroderma treatment has not yet been determined and needs to be examined further.

To determine possible differences between metal-halide lamps and the LED-based UVA_1 prototype on the molecular level, we analysed the gene expression of UVA_1-affected biomolecules involved in scleroderma. Increased MMP-1 expression is one of the most important indicators for successful UVA_1 treatment and significantly improves the clinical condition of LS.[11] MMP-1 is specifically responsible for the breakdown of collagen. Collagen type I (Col-1) is the predominant collagen component of the skin and plays a central role in LS development. Its excessive production by fibroblasts leads to the typical phenotype of dermal fibrosis with accompanying skin hardening due to pathological collagen excess in the dermis. The two biomarkers MMP-1 and Col-1 interact with each other and maintain the balance of collagen metabolism in healthy fibroblasts. UVA_1-induced MMP-1 induction in fibroblasts and the reduction in Col-I has been described in many studies.[32-36] In the present study, we also observed significant MMP-1 induction at the dose of 60 J/cm^2 with either light source and a higher activation rate in fibroblasts irradiated with narrowband LED-based UVA_1. This higher induction capacity of LED-based UVA_1 for MMP-1 maybe a clear advantage of the LED-based UVA_1 light source that potentially results in a better clinical response to treatment. So far, we do not know the mechanism responsible for the higher induction capacity for MMP-1 when using the LED-based UVA_1 lamp. However, comparison of both spectra shows that the LED emission spectrum shows three distinct maxima at about 367, 375 and 385 nm. When neglecting the small peaks, the metal-halide lamp shows five maxima, whereas three maxima can be found in the spectral range of the LED emission spectrum at about 366, 377 and 384 nm. Thus, the maxima in the comparable wavelength show almost the same wavelengths. Besides the small part in the visible spectrum, the major difference of both spectra can be assigned to the short wavelength part of the UVA spectrum. Thus, at equal radiant exposure, the LED-based UVA_1 lamp provides more photons in the short wavelength range from about 360 to 400 nm. A set of molecules in cells like flavins and vitamin A show absorption maximum in the range of 370-380 nm.[37,38] Part of these molecules efficiently generate singlet oxygen which in turn may induce MMP-1.[39,40] This hypothesis is purely speculative and must be investigated in further studies.

In addition to MMP-1 induction, our study also showed reduction in Col-1. Although collagen balance is of particular importance in sclerotic diseases, collagen degradation by UVA_1 treatment plays a relatively minor but not less important role than the induction of MMP-1. In percentage terms, UVA_1 irradiation has a significantly stronger effect on MMP-1 activation than on the reduction in Col-1[32] as confirmed by our study.

In addition to the intervention in the collagen balance of fibroblasts, another important mechanism of UVA_1 irradiation is its immunomodulatory effect. This effect particularly concerns pro-inflammatory cytokines such as IL-1α and IL-6 that signal mediate functions inside and outside a cell. Stimuli of cytokine production in the cells are different stress factors such as exposure to UV light. The synthesis of pro-inflammatory cytokines forms a mutually stimulating network, in which IL-1α plays a special role. IL-1α may influence the collagen metabolism and is a major stimulus for the synthesis of other profibrotic regulatory proteins such as IL-6 or IL-8.[41,42] Kreuter and colleagues described significantly down-regulated mRNA expression of IL-6 and IL-8 after UVA_1 treatment in patients with LS.[43] Vielhaber et al controversially discussed in their study that increased UVA_1-induced MMP-1 production is connected with the upregulation of the cytokine IL-1α and the resulting increase in IL-6 synthesis.[44] Increased IL-1α and IL-6 gene expression after UVA_1 irradiation of fibroblasts was also found by Wlaschek et al[36,40] Any comparison of study results should distinguish between normal fibroblasts and LS-derived fibroblasts. Our study involved normal fibroblasts. Similar to the results of Wlaschek et al,[36,40] we observed a significant induction of IL-1α and IL-6 expression for both UVA_1 light sources. In addition, the growth factors of the TGFß family are considered to be further important indicators for fibrosis and play an essential role in scleroderma. In the dermis, TGFß stimulates the proliferation of dermal fibroblasts, which in turn secrete increased amounts of ECM components such as Col-1 and have a reducing effect on MMP-1 expression.[45-48] In addition, TGFß may suppress the production of IL-1, TNFα and IL-8, which in turn shows the interplay between pro- and anti-inflammatory functions in cytokine-mediated inflammatory reactions.[49] The two most important isoforms of TGFß are TGFß-1 and TGFß-2, both crucial factors in the pathogenesis of fibrosis.[47,50-53] In activated scleroderma fibroblasts, the growth factor TGFß-1 is excessively secreted.[45] In addition, mRNA gene expression of TGFß in lesional skin areas significantly decreases after UVA_1 therapy in patients with LS.[45] Other in vivo studies using normal human skin samples yielded contradictory results. Quan et al described the significant upregulation of TGFß-1 combined with a simultaneous decrease in TGFß-2 after exposure to UV irradiation.[54] In experiments with skin fibroblasts, Yin et al also observed the significant induction of TGFß-1 after UVA treatment.[48] The results of Quan et al and Yin et al[48,54] are also reflected in our study. 24 hours after UVA_1 exposure, TGFß-1 expression was increased simultaneously with reduced TGFß-2 expression in normal fibroblasts.

Effective UVA_1 treatment of scleroderma in vivo decreases dermal thickness primarily due to the degradation and reduction in collagen.[32] In our in vivo experiment, all groups except control group 1 received bleomycin injections and developed the typical picture of the fibrosis mouse model described by Yamamoto et al[20-23] The bleomycin control group 2 clearly showed thicker dermis than groups 3, 4, 5 and 6 that were additionally treated with UVA_1. Also clearly visible were the fat cells displaced by dermal fibrosis that resulted in complete absence of these cells due to highly pronounced fibrosis, especially in control group 2 of this study. Here, fat cells are replaced by fibrotic tissue through adipocyte-myofibroblast transformation.[55,56] Slight regeneration of fatty tissue was observed in the experimental groups treated with UVA_1. Increased myofibroblast activity and associated profibrotic processes significantly contributing to the development of fibrosis[21,57] could be observed in the α-SMA stains of

groups 2-6 treated with bleomycin. Quantification of α-SMA–positive fibroblasts by a dermato-histopathologist showed a decrease in activated myofibroblasts after UVA_1 treatment. Myofibroblasts were significantly reduced compared to the untreated control group 2 after high-dose treatment with the metal-halide lamp (group 3). Interestingly, similar significant effects could be already achieved with a medium dose of the LED-based UVA_1 prototype (group 6). The induction of neoangiogenesis occurring as wound healing process in UVA_1-treated mice could also be observed by means of α-SMA staining, as Trompezinski et al showed in an experimental approach.[28] These α-SMA–stained vascular structures dominate the histological picture of the UVA_1 treated groups and were of course excluded in the quantification of α-SMA–positive myofibroblasts.

Compared to already published results, our histological analysis showed that 30 irradiations (cumulative dose of 3000 J/cm^2) with a high UVA_1 dose (100 J/cm^2) with either light source significantly reduced the dermal diameter by about 25%; the reduction achieved with medium-dose UVA_1 treatment (60 J/cm^2) (cumulative dose of 1800 J/cm^2) was about 20%. These results indicate that both light sources are effective in treating sclerosis and have almost the same effect on reducing dermal thickness. Karpec and colleagues described in their animal study that even a cumulative dose of UVA_1 with a narrowband (365 ± 5 nm) LED-based UVA_1 light source that was 5 times lower than that of conventional broadband UVA_1 lamps had almost the same effect on decreasing dermal thickness (skin thickness was reduced by 34% after irradiation with a cumulative dose of 600 J/cm^2 and by 36% using 3000 J/cm^2).[31] In our similar mouse model, reduction in the dermal diameter in the 129Sv/Ev mouse strain was lower than that achieved by Karpec using two different devices for UVA_1 irradiation. This difference may be due to the different animal strains (129Sv/Ev versus DBA/2), differences in the performance of the bleomycin-induced sclerosis model (maintenance of the sclerosis status versus no further bleomycin treatment during the period of UVA_1 therapy) or the different spectral ranges of the LED source (360-400 nm vs 365 ± 5 nm).

Nevertheless, this study indicates that the two tested UVA_1 light sources are effective in reducing skin sclerosis with similar or even better effects of the new LED light source on the histological and molecular level. In terms of biosafety and patient comfort, the LED-based UVA_1 light source offers clear advantages such as an arrower UVA_1 spectrum, less heat generation and shorter treatment times. Further clinical studies are required to confirm these results in patients with LS or related sclerotic skin diseases such as eosinophilic fasciitis, lichen sclerosus et atrophicus or chronic sclerodermiform graft-versus-host (GvHD) disease, in which UVA_1 phototherapy is also a treatment option.

ACKNOWLEDGEMENTS

The authors acknowledge Dr Robert Sellmeier and Sellas Medizinische Geräte GmbH for providing the UVA_1 devices. We thank Monika Schöll for the linguistic revision of the manuscript.

CONFLICT OF INTEREST

The authors have no conflict of interest to declare.

AUTHOR CONTRIBUTION

SA designed the experiments and carried out the animal study together with CL CL carried out the in vitro experiments together with PU SA and CL wrote the paper. PU performed molecular biological tests and prepared the histological preparations. WB organized the study and together with MB supported the study with photobiological expertise. SK directed the study, performed the histological evaluations and participated in the data analysis and discussion with all other authors. All authors read and approved the final manuscript.

ORCID

Stephanie Arndt https://orcid.org/0000-0003-4724-1955

REFERENCES

[1] R. Buense, M. Bouer, I. A. G. Duarte, *An. Bras. Dermatol.* **2012**, *87*, 63.
[2] M. F. Careta, R. Romiti, *An. Bras. Dermatol.* **2015**, *90*, 62.
[3] O. Distler, A. Cozzio, *Semin. Immunopathol.* **2016**, *38*, 87.
[4] R. Laxer, F. Zulian, *Curr. Opin. Rheumatol.* **2006**, *18*, 606.
[5] T. Herzinger, M. Berneburg, K. Ghoreschi, H. Gollnick, E. Holzle, H. Honigsmann, P. Lehmann, T. Peters, M. Rocken, K. Scharffetter-Kochanek, T. Schwarz, J. Simon, A. Tanew, M Weichenthal, *J. Dtsch. Dermatol. Ges.* **2016**, *14*, 853.
[6] R. Knobler, P. Moinzadeh, N. Hunzelmann, A. Kreuter, A. Cozzio, L. Mouthon, M. Cutolo, F. Rongioletti, C.P. Denton, L. Rudnicka, L.A. Frasin, V. Smith, A. Gabrielli, E. Aberer, M. Bagot, G. Bali, J. Bouaziz, A. Braae Olesen, I. Foeldvari, C. Frances, A. Jalili, U. Just, V. Kahari, S. Karpati, K. Kofoed, D. Krasowska, M. Olszewska, C. Orteu, J. Panelius, A. Parodi, A. Petit, P. Quaglino, A. Ranki, J.M. Sanchez Schmidt, J. Seneschal, A. Skrok, M. Sticherling, C. Sunderkotter, A. Taieb, A. Tanew, P. Wolf, M. Worm, N.J. Wutte, *J. Eur. Acad. Dermatol. Venereol.* **2017**.*31*, 1401,
[7] C. J. Gruss, G. von Kobyletzki, S. C. Behrens-Williams, J. Lininger, T. Reuther, M. Kerscher, P. Altmeyer, *Photodermatol. Photoimmunol. Photomed.* **2001**, *17*, 149.
[8] M. Kerscher, T. Dirschka, M. Volkenandt, *Lancet* **1995**, *346*, 1166.
[9] U. Keyal, A. K. Bhatta, X. L. Wang, *Am. J. Transi Res.* **2017**, *9*, 4280.
[10] P. G. Sator, S. Radakovic, K. Schulmeister, H. Honigsmann, A. Tanew, *J. Am. Acad. Dermatol.* **2009**, *60*, 786.
[11] H. Stege, M. Berneburg, S. Humke, M. Klammer, M. Grewe, S. Grether-Beck, R. Boedeker, T. Diepgen, K. Dierks, G. Goerz, T. Ruzicka, J. Krutmann, *J. Am. Acad. Dermatol.* **1997**, *36*, 938.
[12] J. W. Steger, J. H. Matthews, *J. Am. Acad. Dermatol.* **1999**, *40*, 787.
[13] R. C. W. Su, L. Y. Chong, K. K. Lo, H. Stege, J. Krutmann, *J. Am. Acad. Dermatol.* **1998**, *39*, 517.
[14] T. Gambichler, L. Schmitz, *Front. Med.* **2018**, *5*, 237.
[15] U. Keyal, A. K. Bhatta, X. L. Wang, *Am. J. Transl. Res.* **2017**, *9*, 4280.
[16] T. Gambichler, S. Terras, A. Kreuter, *Clin. Dermatol.* **2013**, *31*, 438.
[17] O. Su, N. Onsun, H. K. Onay, Y. Erdemoglu, D.B. Ozkaya, F. Cebeci, A. Somay, *Int. J. Dermatol.* **2011**, *50*, 1006.
[18] N. R. York, H. T. Jacobe, *Int. J. Dermatol.* **2010**, *49*, 623.
[19] S. Zandi, S. Kalia, H. Lui. **2012**;*17*. http://www.skintherapyletter.com/cutaneous-t-cell-lymphomas/uva1-phototherapy/
[20] T. Yamamoto, *Arch. Dermatol. Res.* **2006**, *297*, 333.
[21] T. Yamamoto, K. Nishioka, *Clin. Immunol.* **2002**, *102*, 77.
[22] T. Yamamoto, K. Nishioka, *Exp. Dermatol.* **2005**, *14*, 81.

[23] T. Yamamoto, S. Takagawa, I. Katayama, K. Yamazaki, Y. Hamazaki, H. Shinkai, K. Nishioka, *J. Investig. Dermatol.* **1999**, *112*, 456.
[24] S. Arndt, P. Unger, M. Berneburg, A. K. Bosserhoff, S. Karrer, *J. Dermatol. Sci.* **2018**, *89*, 181.
[25] T. Mosmann, *J. Immunol. Methods* **1983**, *65*, 55.
[26] S. Arndt, S. Karrer, C. Hellerbrand, A. K. Bosserhoff, *J. Investig. Dermatol.* **1914**, *2019*, e1916.
[27] A. López-De León, M. Rojkind, *J. Histochem. Cytochem.* **1985**, *33*, 737.
[28] S. Trompezinski, I. Pernet, C. Mayoux, D. Schmitt, J. Viac, *Br. J. Dermatol.* **2000**, *143*, 539.
[29] S. Inada, S. Kamiyama, I. Akasaki, K. Torii, T. Furuhashi, H. Amano, A. Morita, *Open Dermatol. J.* **2012**, *6*, 13.
[30] D. Karpec, R. Rudys, L. Leonaviciene, Z. Mackiewicz, R. Bradunaite, G. Kirdaite, A. Venalis, *J. Photochem. Photobiol. B* **2017**, *173*, 448.
[31] D. Karpec, R. Rudys, L. Leonaviciene, Z. Mackiewicz, R. Bradunaite, G. Kirdaite, A. Venalis, *Adv. Med. Sci.* **2018**, *63*, 152.
[32] M. El-Mofty, W. Mostafa, S. Esmat, R. Youssef, M. Bousseila, N. Nagi, O. Shaker, A. Abouzeid, *Photodermatol. Photoimmunol. Photomed.* **2004**, *20*, 93.
[33] J. Krutmann, A. Morita, *J. Invest. Dermatol. Symp. Proc.* **1999**, *4*, 70.
[34] T. Polte, R. M. Tyrrell, *Free Radic. Biol. Med.* **2004**, *36*, 1566.
[35] K. Scharffetter, M. Wlaschek, A. Hogg, K. Bolsen, A. Schotthorst, G. Goerz, T. Krieg, G. Plewig, *Arch. Dermatol. Res.* **1991**, *283*, 506.
[36] M. Wlaschek, K. Bolsen, G. Herrmann, A. Schwarz, F. Wilmroth, P.C. Heinrich, G. Goerz, K. Scharffetter-Kochanek, *J. Invest. Dermatol.* **1993**, *101*, 164.
[37] W. Bäumler, J. Regensburger, A. Knak, A. Felgenträger, T. Maisch, *Photochem. Photobiol. Sci.* **2012**, *11*, 107.
[38] A. Knak, J. Regensburger, T. Maisch, W. Bäumler, *Photochem. Photobiol. Sci.* **2014**, *13*, 820.
[39] K. Wertz, N. Seifert, P. B. Hunziker, G. Riss, A. Wyss, C. Lankin, R. Goralczyk, *Free Radic. Biol. Med.* **2004**, *37*, 654.
[40] M. Wlaschek, J. Wenk, P. Brenneisen, K. Briviba, A. Schwarz, H. Sies, K. Scharffetter-Kochanek, *FEBS Lett.* **1997**, *413*, 239.
[41] S. Akira, T. Hirano, T. Taga, T. Kishimoto, *FASEB J.* **1990**, *4*, 2860.
[42] C. G. Larsen, A. O. Anderson, J. J. Oppenheim, K. Matsushima, *Immunology* **1989**, *68*, 31.
[43] A. Kreuter, J. Hyun, M. Skrygan, A. Sommer, A. Bastian, P. Altmeyer, T. Gambichler, *Br. J. Dermatol.* **2006**, *155*, 600.
[44] G. Vielhaber, S. Grether-Beck, O. Koch, W. Johncock, J. Krutmann, *Photochem. Photobiol. Sci.* **2006**, *5*, 275.
[45] T. Gambichler, M. Skrygan, N. S. Tomi, S. Breuksch, P. Altmeyer, A. Kreuter, *Br. J. Dermatol.* **2007**, *156*, 951.
[46] M. Kubo, H. Ihn, K. Yamane, K. Tamaki, *J. Rheumatol.* **2002**, *29*, 2558.
[47] E. A. Smith, E. C. LeRoy, *J. Invest. Dermatol.* **1990**, *95*, S125-S127.
[48] L. Yin, A. Morita, T. Tsuji, *J. Invest. Dermatol.* **2003**, *120*, 703.
[49] C. A. Dinarello, *Chest* **2000**, *118*, 503.
[50] M. H. Branton, J. B. Kopp, *Microbes Infect.* **1999**, *1*, 1349.
[51] A. Leask, D. J. Abraham, *FASEB J.* **2004**, *18*, 816.
[52] S. Nakerakanti, M. Trojanowska, *Open Rheumatol. J.* **2012**, *6*, 156.
[53] F. Verrecchia, A. Mauviel, *World J. Gastroenterol.* **2007**, *13*, 3056.
[54] T. Quan, T. He, S. Kang, J. J. Voorhees, G. J. Fisher, *J. Invest. Dermatol.* **2002**, *119*, 499.
[55] I. L. Kruglikov, *J. Appl. Aesthetics.* **2016**, *2*, 16.
[56] R. G. Marangoni, T. T. Lu, *Curr Opin Rheumatol.* **2017**, *29*, 585.
[57] K. B. Rao, N. Malathi, S. Narashiman, S. T. Rajan, *J. Clin. Diagnostic Res.* **2014**, *8*, ZC14.

SUPPORTING INFORMATION

Additional supporting information may be found online in the Supporting Information section.

Figure S1. UVA_1-phototherapy equipment.

Figure S2. Total MMP-1 protein in the supernatants of UVA_1-treated fibroblasts.

Table S1. Timeline overview of the mouse study. Bleomycin (Bleo)-injections for 30 d (5 times per week for 6 wk; except for healthy control group 1 treated with PBS). 30 UVA_1-irradiation sessions (5 times per week for 6 wk; except for healthy control group 1 and Bleo control group 2) were followed by 10 additional Bleo injections (1-2 times per week for 6 wk; except for healthy control group 1 treated with PBS) to maintain the sclerosis status.

Table S2. Primers and conditions. Quantitative real-time PCR was conducted with specific sets of primers and conditions as indicated in this table. Ann, annealing temperature; melt, melting temperature.

How to cite this article: Arndt S, Lissner C, Unger P, Bäumler W, Berneburg M, Karrer S. Biological effects of a new ultraviolet A_1 prototype based on light-emitting diodes on the treatment of localized scleroderma. *Exp Dermatol*. 2020;29:1199–1208. https://doi.org/10.1111/exd.14135